

# Robust Imaging from Space

## Adjunct Reference Document #2

### SAR Application Case Studies

This paper presents case studies in the use of SAR technology and demonstrate contributions to the nine National Priorities in the following projects:

#### Contents

<b>1</b>	<b><i>International Forest Carbon Initiative (IFCI): Tasmania National Demonstrator</i></b>	<b>1</b>
<b>2</b>	<b><i>Forest Above Ground Biomass (AGB) estimation using SAR, northern Australia.</i></b>	<b>3</b>
<b>3</b>	<b><i>Mapping wetland inundation patterns</i></b>	<b>6</b>
<b>4</b>	<b><i>Flood disaster response: QLD/NSW flood monitoring using SAR</i></b>	<b>8</b>
<b>5</b>	<b><i>InSAR and deformation monitoring arising from Sichuan earthquake, China.</i></b>	<b>9</b>
<b>6</b>	<b><i>Subsidence monitoring using Persistent Scatterer Interferometry (PSI)</i></b>	<b>10</b>
<b>7</b>	<b><i>Modelling of landforms using InSAR DEMs</i></b>	<b>12</b>
<b>8</b>	<b><i>Civilian and Defence Maritime surveillance</i></b>	<b>13</b>
<b>9</b>	<b><i>The Australian Antarctic Division (AAD) mapping program</i></b>	<b>15</b>



#### *Acknowledgements*

These case studies represent the efforts and outcomes of consulting assignments undertaken by leading Australian experts in the field of Synthetic Aperture Radar technologies and applications. Any references to this material should acknowledge the authors and papers referenced.

# Robust Imaging from Space

## Table of Figures

Figure 1 - At left ALOS PALSAR mosaic for Tasmania (2009), at right Derived forest/non-forest map .....	1
Figure 2 - At left: Tasmania 2007 land cover map;. at right:Tasmanian Vegetation Map .....	2
Figure 3 - TOTAL AGLB for eastern Australia as estimated from ALOS PALSAR L-HV and relationships with field data .....	4
Figure 4 - Changes in forest structure detected between 1995 and 2009 using a time-series of JERS-1 and ALOS PALSAR data .....	5
Figure 5 - Multi-temporal RADARSAT colour composite of the South Alligator River region, northern Australia, at right, derived wetland inundation map .....	6
Figure 6 - South Alligator River region, northern Australia, derived wetland inundation map .....	6
Figure 7 - Integration of L-band ALOS PALSAR and X-band TerraSAR-X for discrimination of flooded and non-flooded wetlands. ....	7
Figure 8 - Flooding in Rockhampton, Queensland.....	8
Figure 9 - Ground displacement map and location of aftershocks in China.....	9
Figure 10 - Land Deformation in Sydney due to groundwater extraction.....	10
Figure 11 - Finke River Gorge, James Ranges, Central Australia – DEM generation from airborne C-band radar interferometry. ....	12
Figure 12 - Ship detection using TerraSAR-X imagery.....	13
Figure 13 - Detection of ship’s wake (Kelvin wake) using RADARSAT-1 data .....	13
Figure 14 - Montara oil spill in Timor Sea 2009 .....	14
Figure 15 - 3D perspective model of Macquarie Island: AISAR data overlain on TOPSAR DEM.....	15
Figure 16 - Active microwave data are used in glaciology studies, topographic mapping and change detection .....	16

---

## 1 International Forest Carbon Initiative (IFCI): Tasmania National Demonstrator

National drivers: Agriculture Forestry and Ecosystems; Climate Change, National Mapping

In May 2008, the Australian Government launched the International Forest Carbon Initiative (IFCI) and established the Global Carbon Monitoring System (GCMS), a key requirement to achieving monitoring, reporting and verification objectives of IFCI. Through GCMS, a global network of consistent and compatible national forest monitoring systems that meet national reporting requirements and that could be linked to support carbon trading initiatives was envisioned.

*Under the GEO Forest Carbon Tracking Task (FCT; <http://www.geo-fct.org/>), Tasmania was selected as Australia's National Demonstrator site to undertake activities towards continuous improvement of a globally-applicable methodology combining satellite and in situ data for development of the Australian GCMS. Partnership between the CRC-SI and CSIRO led to the generation of wall-to-wall time-series SAR mosaics, forest/non-forest maps (Figure 1 and Figure 2), land use/land cover and change products, interoperable optical-radar forest monitoring strategies and standardised verification procedures.*

**Reference:** Mitchell, A.L., Milne, A.K., Tapley, I., Lowell, K., Caccetta, P., Lehmann, E., Zhou, Z-S. and Held, A. 2011. Key outcomes of the Tasmania National Demonstrator: a project for the GEO forest carbon tracking task. Proceedings of the 34<sup>th</sup> International Symposium on Remote Sensing of Environment, held in Sydney, April 10-15.

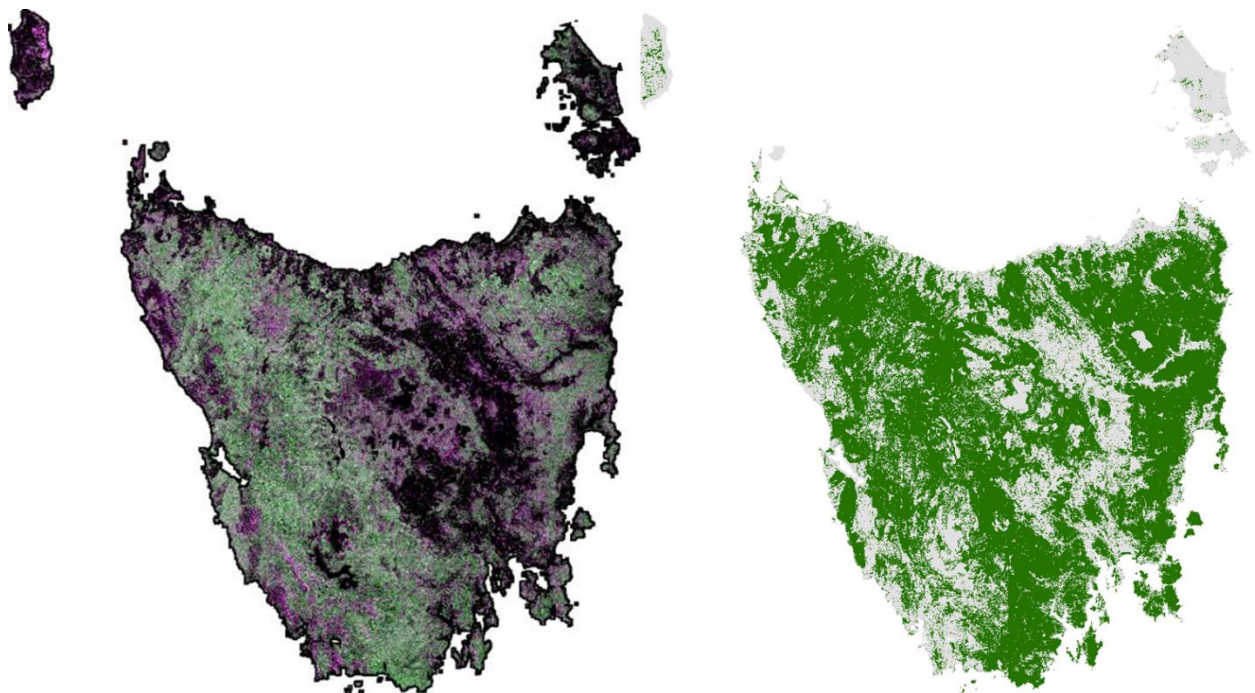


*Figure 1 - At left ALOS PALSAR mosaic for Tasmania (2009), at right Derived forest/non-forest map*

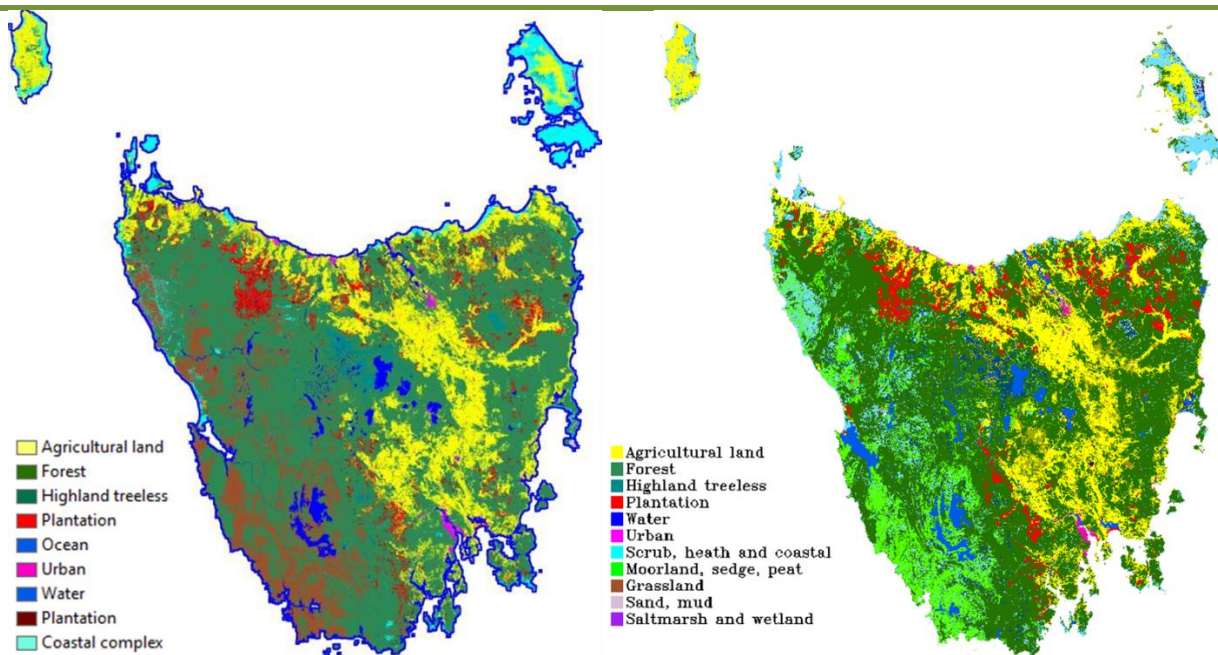


*Figure 2 - At left: Tasmania 2007 land cover map;. at right:Tasmanian Vegetation Map*

## 2 Forest Above Ground Biomass (AGB) estimation using SAR, northern Australia.

### National drivers: Agriculture Forestry and Ecosystems; Climate Change

Deforestation is occurring at a rate of around 13 million hectares per year: an area about 50 times the size of Luxembourg or 180 times the size of Singapore (FAO, 2007). As well as being a major cause of biodiversity loss, tropical deforestation also results in the release of (mostly) carbon dioxide: a major contributor to climate change.

Improved observation of forest and land cover change, including changes in Above Ground Live Biomass (AGLB), will provide valuable input to countries' Monitoring, Reporting and Verification (MRV) systems and future climate change policies focusing on reducing deforestation emissions from developing countries (REDD+). AGLB is recognized as an essential climate variable in emissions accounting from forest and land cover change. Using SAR data, the AGLB of forests has been retrieved through statistical relationships with ground data or interferometric measurements of height.

As an example, ongoing research in Queensland, Australia, has investigated relationships between the ALOS PALSAR L-HH and HV backscattering coefficient and field measured AGB (Lucas et al., 2010a). The relationships were found to be consistent within different structural formations (forests, woodlands and open woodlands). L-band HV increased asymptotically with AGB up to 260 Mg ha<sup>-1</sup> for forests, while in woodlands and open woodlands, saturation of HV occurred at 50-60 Mg ha<sup>-1</sup>. Soil moisture had a significant effect on biomass estimates at L-band, and it was concluded that PALSAR data acquired with minimal soil moisture and rainfall would permit better estimation of AGB over large areas. An interim AGB map for eastern Australia (Figure 3) has been generated and is currently undergoing validation and further improvements are being developed through integration of PALSAR data with Landsat and IceSAT data products.

The successful application of SAR for wide-area AGB estimation across Queensland State is encouraging for routine implementation and national carbon accounting, both in Australia and elsewhere. Time-series radar also facilitates detection and mapping of various levels of forest degradation, regrowth and recovery over large areas (Figure 3; Lucas et al., 2010b).

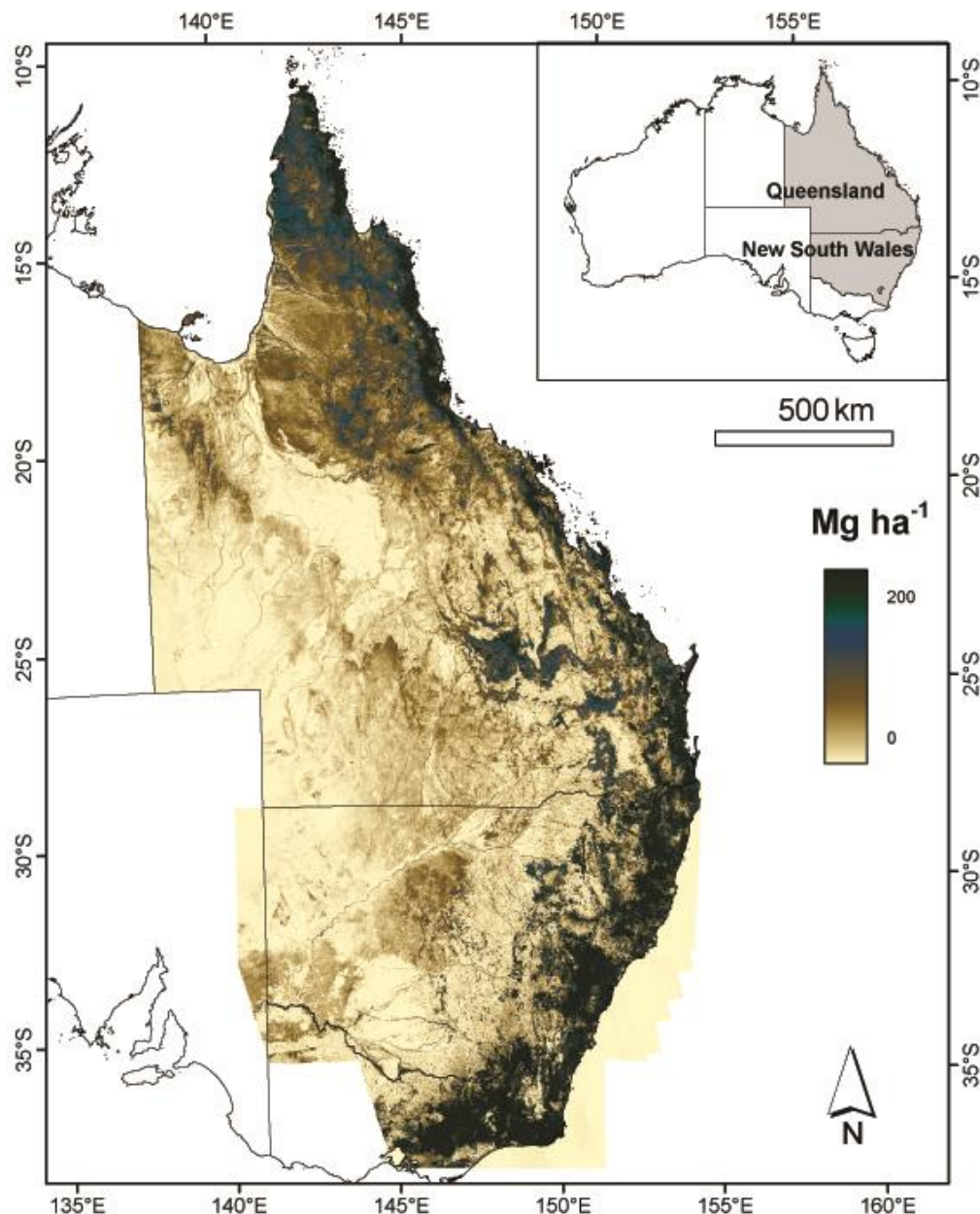


Figure 3 - TOTAL AGLB for eastern Australia as estimated from ALOS PALSAR L-HV and relationships with field data

(Reference: Lucas, R., Armston, J., Fairfax, R., Fensham, R., Accad, A., Carreiras, J., Kelley, J., Bunting, P., Clewley, D., Bray, S., Metcalfe, D., Dwyer, J., Bowen, M., Eyre, T., Laidlaw, M. and Shimada, M. 2010a. An evaluation of the ALOS PALSAR L-band-Above ground biomass relationship Queensland, Australia: Impacts of surface moisture condition and vegetation structure. *IEEE Journal of Selected Topics in Applied Earth Observations and Remote Sensing*, 3,4: 576-593). This work has been undertaken [in part] within the framework of the JAXA Kyoto & Carbon Initiative. ALOS PALSAR data have been provided by JAXA EORC.

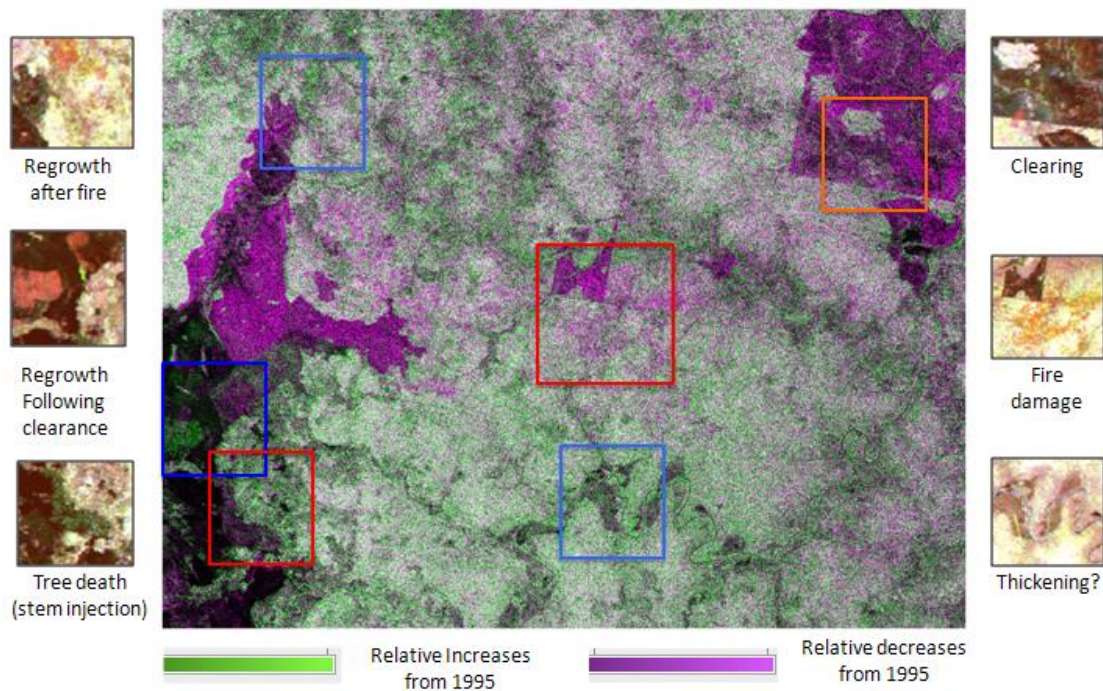


Figure 4 - Changes in forest structure detected between 1995 and 2009 using a time-series of JERS-1 and ALOS PALSAR data

(Reference: Lucas, R., Bunting, P., Armston, J., Lee, A. and Campbell, G. 2010b. The Injune Collaborative Project: An update on research activities. Proceedings of the 15th Australasian Remote Sensing and Photogrammetry Conference, Alice Springs, NT, Sept 13-17).

*This work has been undertaken [in part] within the framework of the JAXA Kyoto & Carbon Initiative. ALOS PALSAR data have been provided by JAXA EORC.*

### 3 Mapping wetland inundation patterns

#### National drivers: Climate Change; Water Availability

The use of a time series of radar images collected throughout a seasonal cycle provides the potential for mapping wetland units and monitoring seasonal changes in the landscape on a regional basis. Figure 5 shows multi-temporal, Radarsat C-band HH-polarization colour-composite change image of 3 registered 1998 scenes (30 m pixels) of the South Alligator River region, northern Australia. Landscape features that do not appear in single-date images become visible and the relative changes that these features undergo infer fine boundaries between ecological classes. Blue represents areas that have dried out first between February and May; Green represents areas dried out between May and September; Red areas are still saturated and covered with macrophytes or active flooded grasslands. White are permanently flooded swamplands. Black represents open water, while pink show areas of higher land tree cover.

**Reference:** Milne, A.K., Horn, G. and Finlayson, M., 2000. [Monitoring wetlands inundation patterns using Radarsat multi-temporal data.](#) *Canadian Journal of Remote Sensing*, Vol. 26, No. 2, April 2000.



Reliable spatial information is required to guide the targeting of environmental flows and assess the ecological outcomes of water distribution in wetlands. In a pilot study undertaken by Milne et al. (2008), the capacity of imaging radar to map and monitor wetland extent and inundation in the Macquarie Marshes in north central NSW was demonstrated. The study highlighted the benefits of incorporating SAR in an operational system for monitoring environmental flows and wetland dynamics in the Macquarie Marshes and other significant wetlands.

*Figure 5 - Multi-temporal RADARSAT colour composite of the South Alligator River region, northern Australia, at right, derived wetland inundation map*

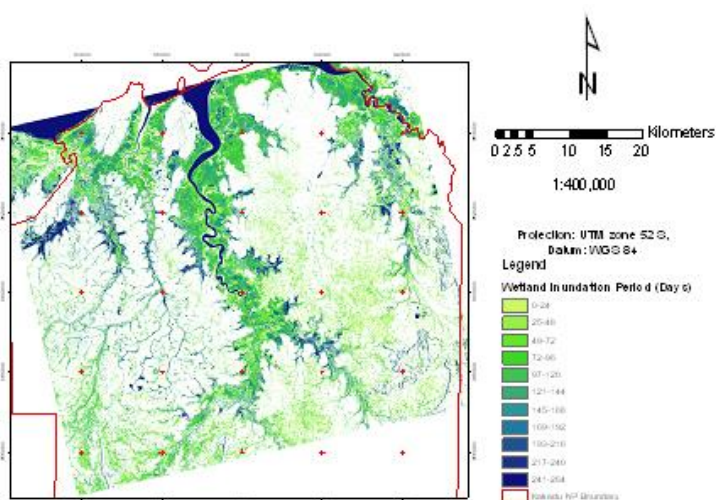


*Figure 6 - South Alligator River region, northern Australia, derived wetland inundation map*

A combination of L-band ALOS PALSAR and X-band TerraSAR-X data provides good discrimination of wetland surfaces (Figure 7). The backscatter over the floodplain wetland is dominated by the PALSAR Mar08 response (green on image). This is due largely to the L-band response to high soil moisture and roughness. The backscatter over the surrounding floodplain area is dominated by the TSX Mar08 response (purple on image). The low shrubs and grasses of the floodplain provide many opportunities for volume scattering at X-band. Patches are observed in the edge wetland where the response is also dominated by the TSX Mar08 image. These are most likely areas of very high backscatter as a result of ponded water with aquatic vegetation.

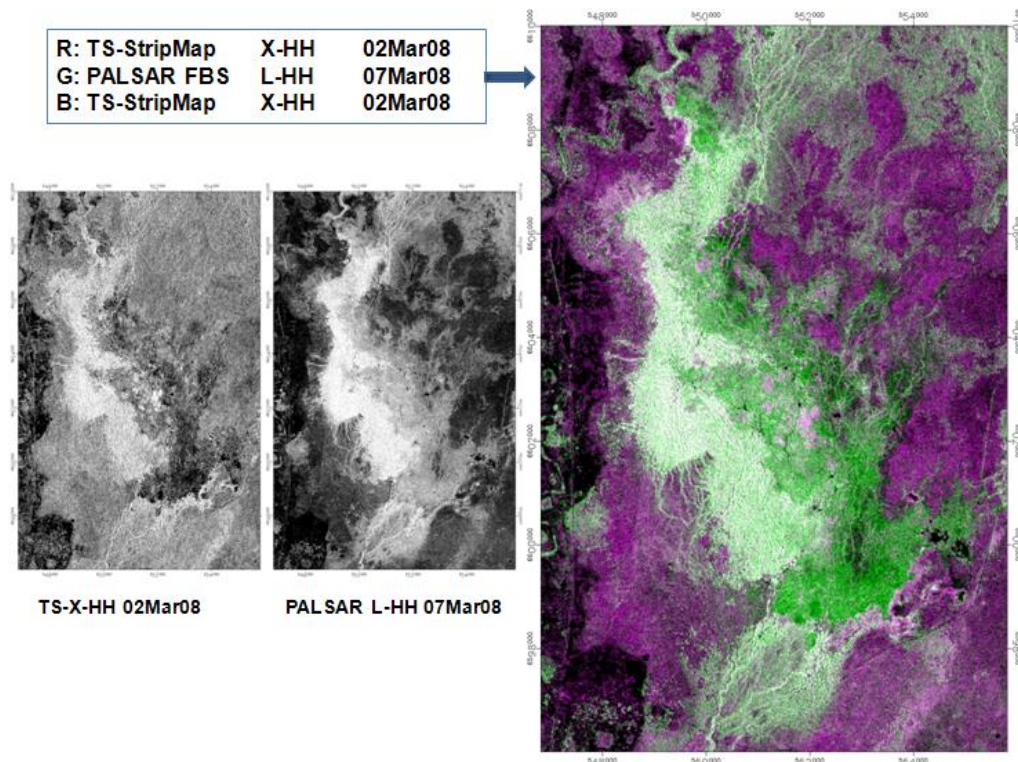


Figure 7 - Integration of L-band ALOS PALSAR and X-band TerraSAR-X for discrimination of flooded and non-flooded wetlands.

The TerraSAR-X data provide a first surface return or largely canopy response. Dark areas on the floodplain at X-band reveal areas where the water has overtopped the vegetation in the wetlands. The PALSAR data respond to woody vegetation, particularly where inundated and provide good discrimination between flooded and non-flooded vegetation.

**Reference:** Milne, A.K., Tapley, I., Mitchell, A.L. and Powell, M. 2008. Trial of L-band radar for mapping inundation patterns in the Macquarie Marshes. Research report prepared for the NSW Department of Environment and Climate Change (DECC), Dec 2008.

## 4 Flood disaster response: QLD/NSW flood monitoring using SAR

### National drivers: Natural Disaster Mitigation

Under the influence of Cyclone Tasha and La Nina, the December 2010 - January 2011 flood events brought widespread devastation to vast extents of eastern Australia, particularly Queensland. There was varied use of spatial information including satellite radar imagery in post-disaster response activity. A case study on the effective use of spatial information in the flood response can be found at:

<http://www.crcsi.com.au/Research/Commissioned-Research/Spatial-information-for-disaster-response>.

Radar's all-weather, cloud penetrating, day/night observation capability renders it a viable tool in flood emergency response and pre- and post-flood extent mapping and ground operations. The ability to capture useful imagery over extensive areas during heavy cloud days when aerial imagers cannot is invaluable.

During the 2010/11 flood event, radar imagery acquired by Cosmo-SkyMed, TerraSAR-X and RADARSAT-2 were used primarily to map flood extents (Figure 8), inform disaster recovery activities, and support high-level response planning. The high resolution of the radar imagery and accuracy of mapped flood zones was deemed useful in its own right and as a useful complement to aerial imagery in building situational awareness during the flood event. The main limitations in the use of SAR were the latency in obtaining the data and lack of familiarity with the data and products.

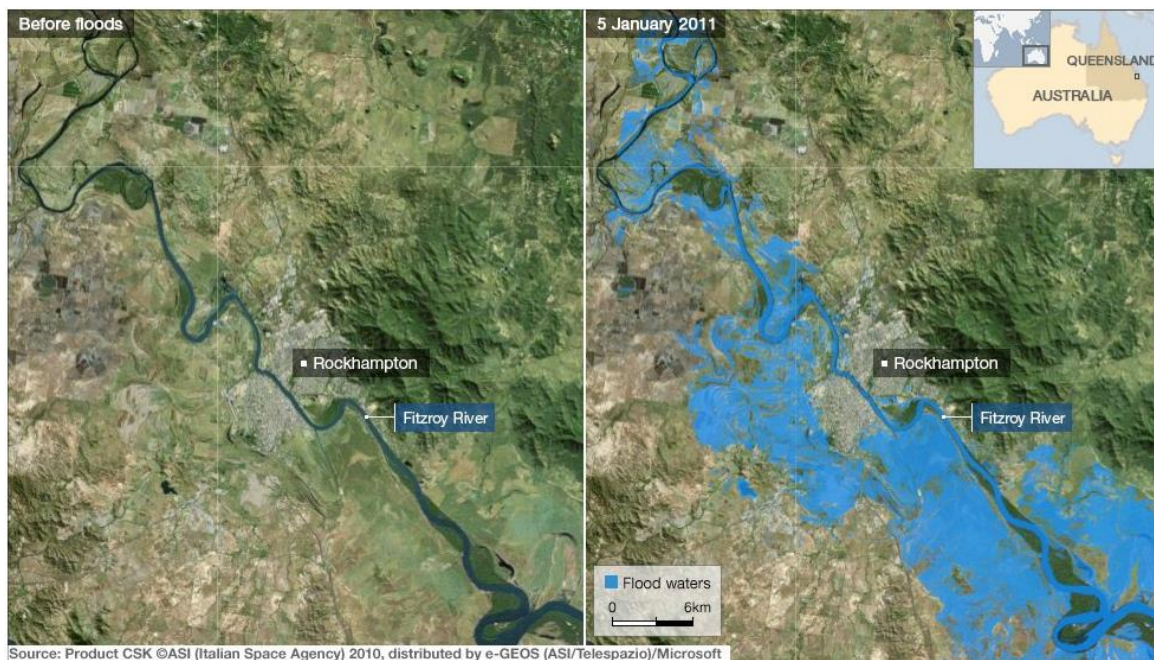


Figure 8 - Flooding in Rockhampton, Queensland

- Left -Optical image taken prior to flooding, and
- Right- Radar derived (Cosmo-SkyMed) flood extent map for 5 Jan 2011 overlain on optical image. (Geodesy and Earth Observing Systems Group, University of NSW, Source: <http://www.bbc.co.uk/news/world-asia-pacific-12138010>).

## 5 InSAR and deformation monitoring arising from Sichuan earthquake, China.

### National driver: Natural Disaster Mitigation

A devastating magnitude 8.0 earthquake struck Sichuan, China in May 2008. To assist with disaster response efforts, researchers from the CRC for Spatial Information (UNSW) in collaboration with agencies in Japan and China provided near real time ground displacement maps of the earthquake zone to Chinese authorities to assist in identifying where deployment of rescue teams would be most effective and where aftershocks and landslides were likely (Figure 9). Ground displacement maps were generated using imagery from JAXA's ALOS PALSAR satellite. Deformation of up to 5 m was measured using radar interferometry techniques, providing critical spatial information on ground movements and potential for landslip and damage to buildings and urban infrastructure.

In 2007, CRC-SI established a research agreement with China's Centre for Earth Observation and Digital Earth at the Chinese Academy of Sciences to strengthen capacity for earth observation in relation to ground displacement. Future radar satellites to be launched by China will provide valuable information for monitoring and predicting ground and slope changes for early warning and evacuation response. The contribution of Assoc Prof Linlin Ge and his team was recognized by the highest Asia-Pacific Spatial Excellence Award for 2008.

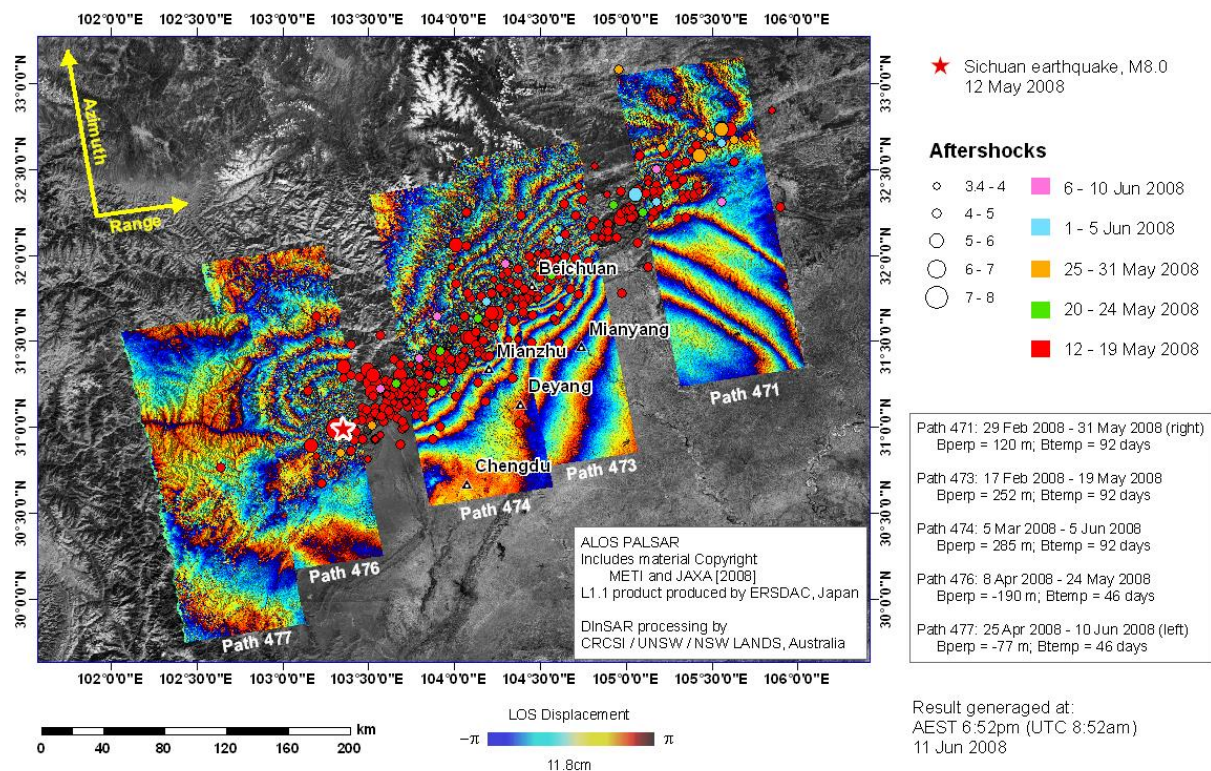


Figure 9 - Ground displacement map and location of aftershocks in China.

(Source: <http://www.gmat.unsw.edu.au/LinlinGe/Earthquake/>).

## 6 Subsidence monitoring using Persistent Scatterer Interferometry (PSI)

### National drivers: Energy and Resource Security

PSI makes measurements of ground movement on naturally occurring permanent scattering points such as the roofs of buildings, metallic structures and prominent natural features. In urban areas, there can be several hundred persistent scatterers per square kilometre. Uniquely, this technique provides the motion history (for the period of the data archive which can be 10 or so years) for each individual persistent scatterer. Atmospheric artefacts and topographic induced errors are overcome by typically utilising 30 or more scenes to identify a dense network of pre-existing permanent scatterers that provide strong backscatter reflection to the spaceborne SAR. With this array of points, movement of individual or clusters of scatterers can be measured with millimetre accuracy. It must be realized that the measured movement of a permanent scatterer is of the scatterer itself, not the ground but the two are obviously interrelated.

PSI is an InSAR technique ideally suited to observations in urban and semi-urban areas of surface changes where point scatterers are abundant. If additional reflectors are required in zones or towards the edges of urban scenes where numbers of natural reflectors are less than desirable then artificial radar reflectors can be installed. An ongoing application of PSI is for monitoring ground subsidence due to groundwater extraction from local aquifers and mining subsidence (Figure 10). Both PSI and DInSAR techniques can be used to measure displacements arising from these activities.

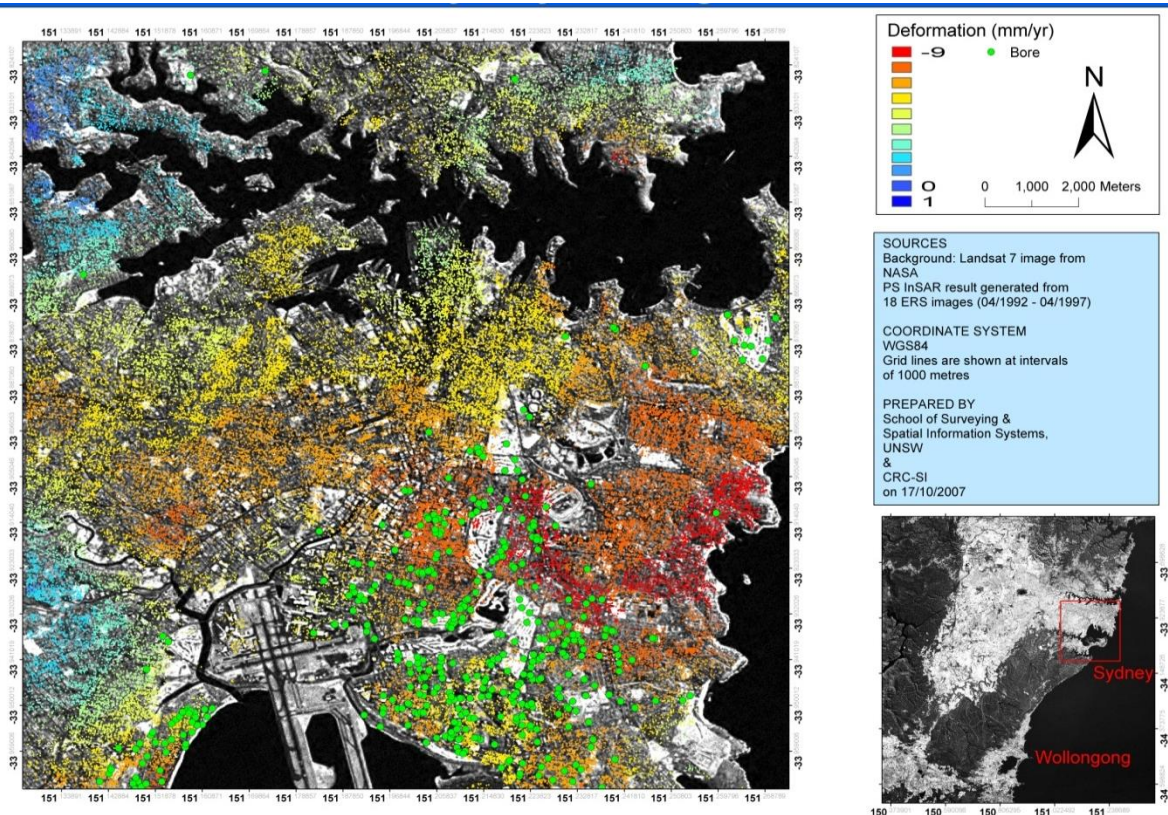


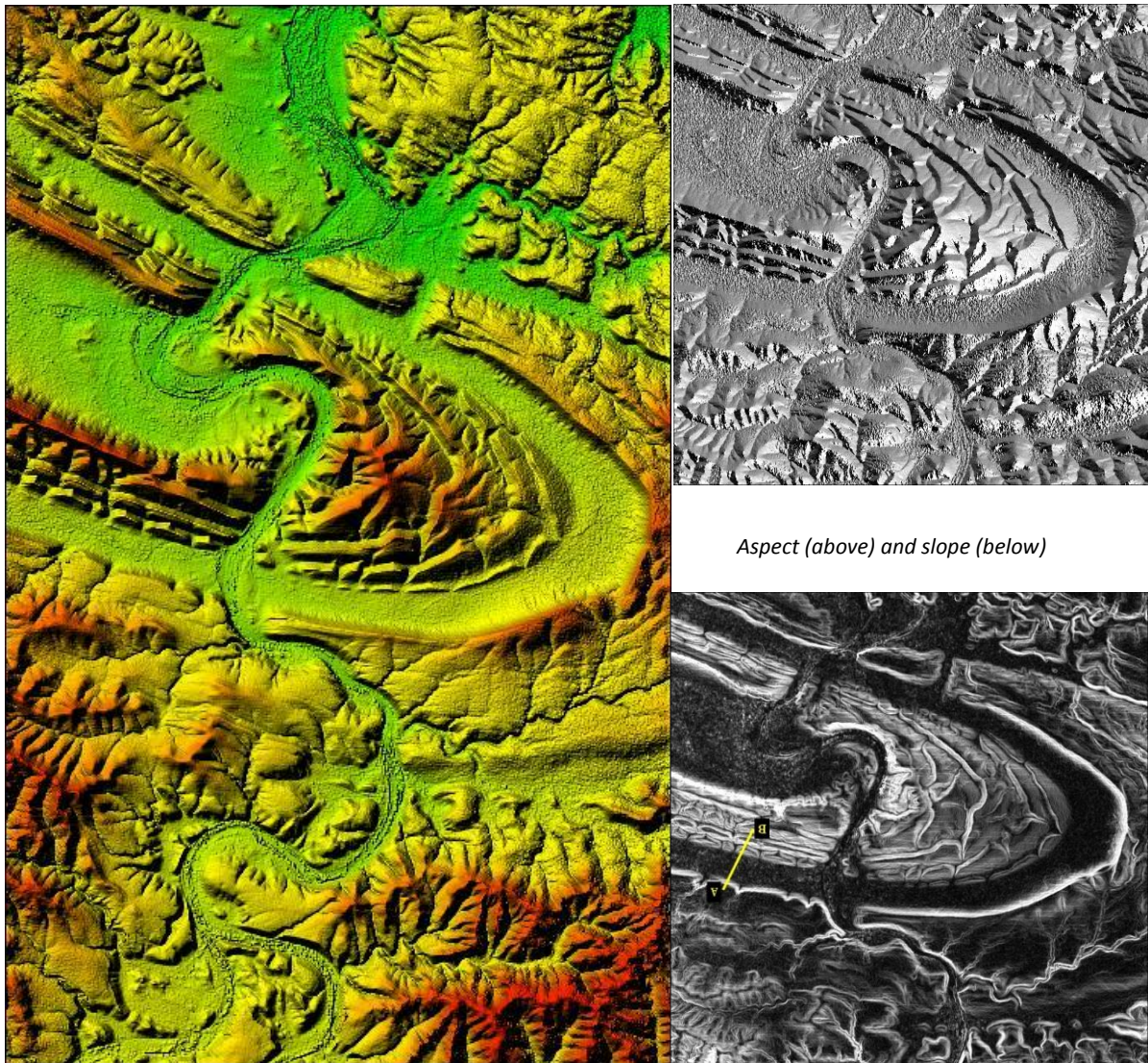
Figure 10 - Land Deformation in Sydney due to groundwater extraction.

Application of Persistent Scatterer Interferometry to examine subsidence of Sydney over period April 1992 to April 1997 using 18 ERS radar scenes. The location points of the many thousands of permanent scatterers are colour-coded according to the subsidence measured for the 6 year period. The highest deformation rate (colour Red) is up to -9mm/year, located in the Eastern Suburbs over a principal groundwater site, the Botany Sands aquifer. **Reference:** Ng, A.H-M. and Ge, L., 2007. Application of persistent scatterer in InSAR and GIS for urban subsidence monitoring. *IEEE Int. Geoscience & Remote Sensing Symposium, Barcelona, Spain, 23- 27 July, paper 1296.*

## 7 Modelling of landforms using InSAR DEMs

### National drivers: National Mapping

DEMs are essential for landform analysis and for understanding and quantifying hydrological processes associated with floods, water run-off, and sediment transport as preparation for and mitigating natural disasters and managing landuse - especially when studying regions where the collection of optical data for the generation of DEMs is hindered by local climatic conditions. Dip and strike slopes of the folded sandstone sequence can be readily observed using airborne and spaceborne SAR (Figure 11). Strike ridges and valleys, steeply-dipping fold sequences and drainage divides are highlighted by the shaded-relief (12x20 km) and vertical derivative models (12x12 km) derived from the InSAR data which have a 5x5 m spatial resolution, height accuracy of <1-3 m depending on terrain type, and height relief of 341 (green) – 891 m (red);



*Aspect (above) and slope (below)*

*Figure 11 - Finke River Gorge, James Ranges, Central Australia – DEM generation from airborne C-band radar interferometry.*

(Source: [Horizon Geoscience Consulting](#)).

## 8 Civilian and Defence Maritime surveillance

### National drivers: Safe and Secure Transport, Coasts and Oceans, National Security

Australia's Coastwatch program employs satellite technology for national maritime surveillance. SAR is most useful during long periods of heavy cloud cover which negate the use of optical satellites. Radar data from satellites such as RADARSAT-1 are being used to locate relatively large ships and track their movements over a number of days. Satellites are also used for surveillance in areas such as Cocos Islands, Christmas Island and other offshore areas. Australian Defence and Customs have trialed the use of High Frequency Surface Wave Radar (HFSWR) to detect surface vessels and low-flying aircraft. This has potential to provide 24-hour wide-area coastal surveillance of aircraft, ships and boats travelling in the Torres Strait. Unmanned Aerial Vehicles (UAV) with various imaging payloads are also used for prolonged surveillance to identify and verify targets detected from HFSWR and other sources

(Source: [http://www.customs.gov.au/webdata/minisites/annualreport0405/performance/output\\_3\\_maritime\\_surv.html](http://www.customs.gov.au/webdata/minisites/annualreport0405/performance/output_3_maritime_surv.html)).

SAR X-band, C-band and potentially S-band imagery offers the most appropriate specifications suited to this application area.

Radar data from satellites such as TerraSAR-X and Radarsat are being used to locate relatively large ships and track their movements over a number of days. Ships can be detected through direct measurement of backscatter from reflective surfaces using:

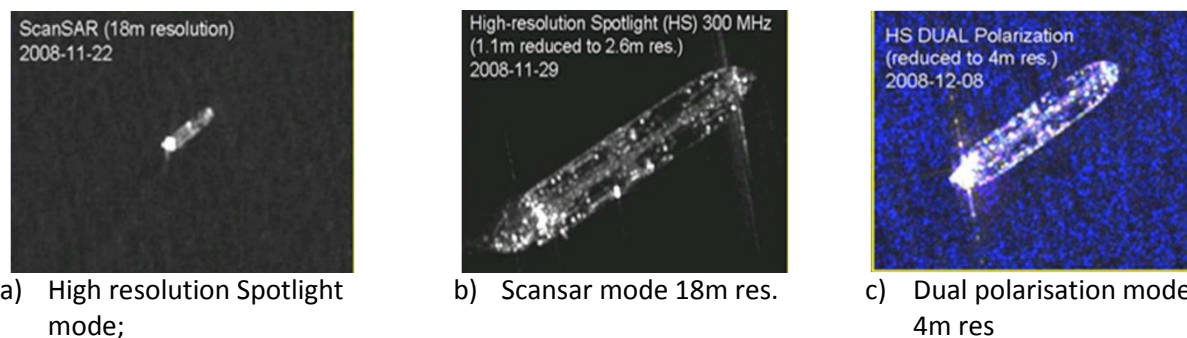
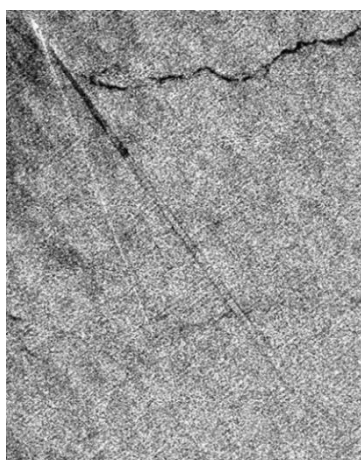


Figure 12 - Ship detection using TerraSAR-X imagery

**Reference:** Brusch, S., Lehner, S., Fritz, T., Soccorsi, M., Soloviev, A., and van Schie, S. Ship Surveillance with TerraSAR-X, *IEEE Transaction of Geoscience and Remote Sensing*, vol 49, no 3, March 2011, pp.1092-1103.



Ships can be detected through direct measurement of backscatter from reflective surfaces or indirectly by detecting the ship's wake. Measurements of a ship's direction and speed from SAR imagery must be available as soon as possible after the satellite overpass to be useful for intervention measures.

The ship's wake creates turbulence and areas of smoother water that stand out from the surrounding ocean in a SAR image. The bow of a ship when pushing the water aside also creates a wave known as the Kelvin wake (Figure 13). This wave emanates from either side of the bow and forms a distinct part of the ship's SAR signature.

Figure 13 - Detection of ship's wake (Kelvin wake) using RADARSAT-1 data

Source: [www.ga.gov.au/ausgeonews/ausgeonews200809/satellite.jsp](http://www.ga.gov.au/ausgeonews/ausgeonews200809/satellite.jsp)

*On 21 August 2009, the Montara offshore oil platform in the Timor Sea started leaking oil. Over a period of ten weeks, more than two million litres of oil were lost into the sea, forming a 2000 square kilometre slick.*

This TerraSAR-X image (Figure 14) at right, was acquired by Astrium on 21 September 2009 in ScanSAR mode. The resolution is 18 metres and the image covers an area of 100 by 150 kilometres. The oil well was closed at the beginning of November.

Australia currently has no dedicated satellite surveillance capability, although Defence has capacity to access classified allied satellite intelligence (Bateman 2007)<sup>1</sup>.

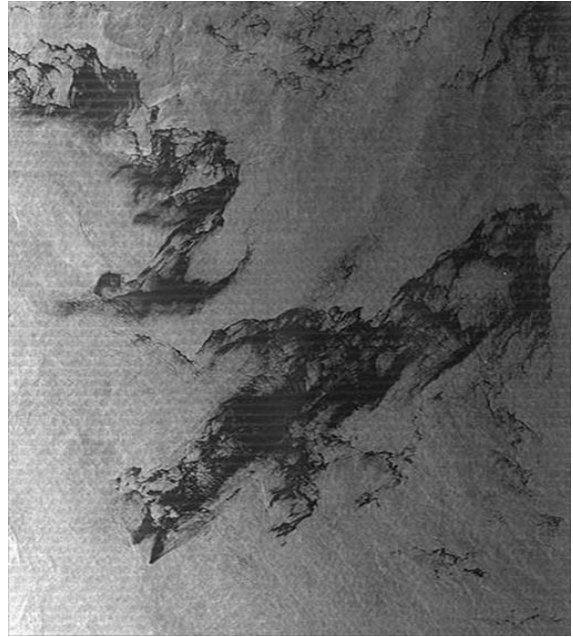


*Figure 14 - Montara oil spill in Timor Sea 2009*

Source: DLR Web Portal News Archive - TerraSAR-X image of the month: Oil disaster off the Australian coast 27 Nov 2009 ([http://www.dlr.de/en/desktopdefault.aspx/tabid-6214/10201\\_read-20853](http://www.dlr.de/en/desktopdefault.aspx/tabid-6214/10201_read-20853))

---

<sup>1</sup> Reference: Bateman, S. - *Securing Australia's Maritime Approaches. Security Challenges*, 3, 3: 109-129.

## 9 The Australian Antarctic Division (AAD) mapping program

National drivers: Climate Change; Coasts and Oceans, Safe and Secure Transport.

The AAD are committed to ongoing scientific investigation of the Antarctic mainland and surrounding sub-arctic island between Australia and Antarctica, EOS data is an essential component of routine mapping and monitoring activity in Antarctica. Spaceborne passive sensors provide daily updates for sea ice-covered regions important for navigation and safe passage.

SAR data are used in glaciology studies, topographic mapping and change detection. AIRSAR data acquired over Macquarie Island in 2000 as part of the NASA/Australian AISAR PACRIM Mission has been used to construct the first complete topographic map of the island and to study tectonic movements associated with plate boundary movements and re-activated sea floor structures along the islands coastline.

Active microwave data are used in glaciology studies, topographic mapping and change detection (Figure 15 and Figure 16).

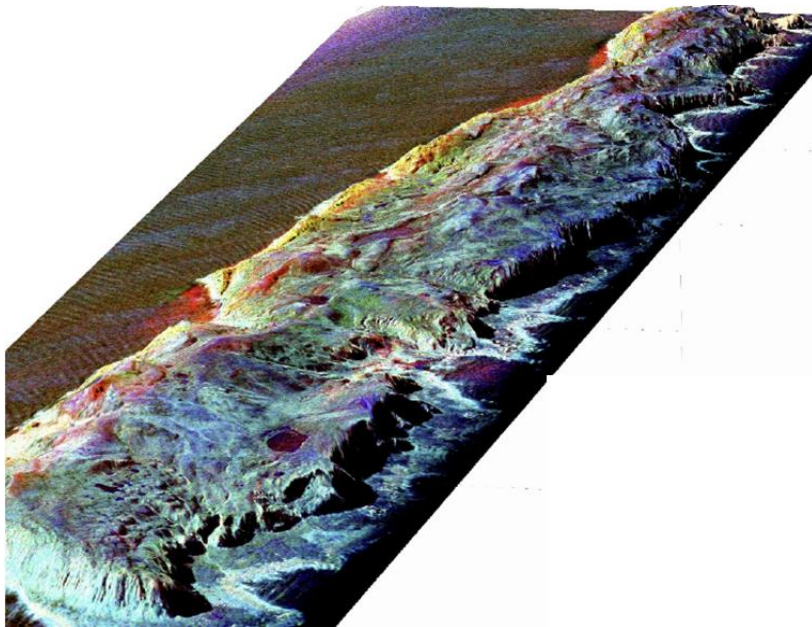


*Figure 15 - 3D perspective model of Macquarie Island: AISAR data overlain on TOPSAR DEM.*

(R: P pedestal height, G: L pedestal height, B: C-VV) viewed from NNW (Tapley et al., 2004)

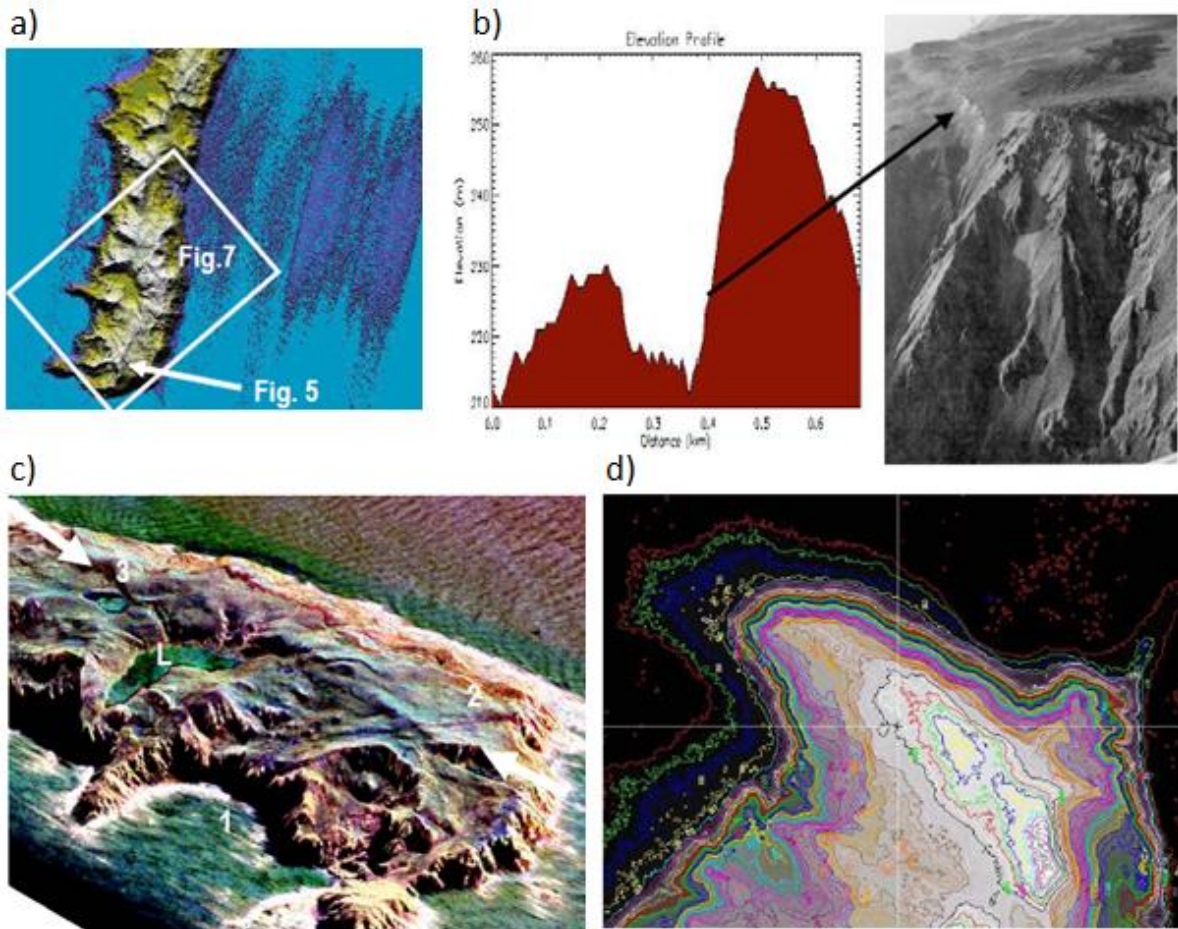


Figure 16 - Active microwave data are used in glaciology studies, topographic mapping and change detection

- a) Location diagram of Macquarie Island;
- b) Height profile of steeply inclined fault scarp relating to (a);
- c) 3D image showing circular features near Caroline Cove (1), Hurd Point Fault Zone (2) and a degraded NS scarp (3) along middle of island, relating to (a); and
- d) 5m height contours on northern coastline generated from TOPSAR interferometry (Tapley et al., 2004).

**Reference:** Tapley, I., Dijkstra, A.H. and Broksma, H. 2004. The geology, landforms and topography of sub-Antarctic Macquarie Island, Australia, as revealed by AIRSAR. *Proceedings of the IEEE Geoscience and Remote Sensing Symposium*, 1: 649-652.